



## Nanostructured hybrid hydrogels prepared by a combination of atom transfer radical polymerization and free radical polymerization

Sidi A. Bencherif<sup>a</sup>, Daniel J. Siegwart<sup>b</sup>, Abiraman Srinivasan<sup>c</sup>, Ferenc Horkay<sup>d</sup>, Jeffrey O. Hollinger<sup>c</sup>, Newell R. Washburn<sup>a</sup>, Krzysztof Matyjaszewski<sup>a,\*</sup>

<sup>a</sup>Department of Chemistry, Carnegie Mellon University, Pittsburgh, PA 15213, USA

<sup>b</sup>Department of Chemical Engineering, Massachusetts Institute of Technology, Cambridge, MA 02139, USA

<sup>c</sup>Bone Tissue Engineering Center, Carnegie Mellon University, Pittsburgh, PA 15219, USA

<sup>d</sup>Section on Tissue Biophysics and Biomimetics, Laboratory of Integrative and Medical Biophysics, NICHD, National Institutes of Health, Bethesda, MD 20892, USA

### ARTICLE INFO

#### Article history:

Received 3 April 2009

Accepted 8 June 2009

Available online 9 July 2009

#### Keywords:

Hydrogels

Nanogels

Hyaluronic acid

Hybrid

Atom transfer radical polymerization (ATRP)

Free radical photopolymerization (FRP)

### ABSTRACT

A new method to prepare nanostructured hybrid hydrogels by incorporating well-defined poly(oligo (ethylene oxide) monomethyl ether methacrylate) (POEO<sub>300</sub>MA) nanogels of sizes 110–120 nm into a larger three-dimensional (3D) matrix was developed for drug delivery scaffolds for tissue engineering applications. Rhodamine B isothiocyanate-labeled dextran (RITC-Dx) or fluorescein isothiocyanate-labeled dextran (FITC-Dx)-loaded POEO<sub>300</sub>MA nanogels with pendant hydroxyl groups were prepared by activators generated electron transfer atom transfer radical polymerization (AGET ATRP) in cyclohexane inverse miniemulsion. Hydroxyl-containing nanogels were functionalized with methacrylated groups to generate photoreactive nanospheres.

<sup>1</sup>H NMR spectroscopy confirmed that polymerizable nanogels were successfully incorporated covalently into 3D hyaluronic acid-glycidyl methacrylate (HAGM) hydrogels after free radical photopolymerization (FRP). The introduction of disulfide moieties into the polymerizable groups resulted in a controlled release of nanogels from cross-linked HAGM hydrogels under a reducing environment. The effect of gel hybridization on the macroscopic properties (swelling and mechanics) was studied. It is shown that swelling and nanogel content are independent of scaffold mechanics. *In-vitro* assays showed the nanostructured hybrid hydrogels were cytocompatible and the GRGDS (Gly–Arg–Gly–Asp–Ser) contained in the nanogel structure promoted cell–substrate interactions within 4 days of incubation. These nanostructured hydrogels have potential as an artificial extracellular matrix (ECM) impermeable to low molecular weight biomolecules and with controlled pharmaceutical release capability. Moreover, the nanogels can control drug or biomolecule delivery, while hyaluronic acid based-hydrogels can act as a macroscopic scaffold for tissue regeneration and regulator for nanogel release.

© 2009 Elsevier Ltd. All rights reserved.

### 1. Introduction

The design of polymer hydrogels with new properties has attracted a great deal of interest in pharmaceutical and biomedical fields because of their 3D physical structure, mechanical properties, high water content, and biocompatibility [1,2]. These compelling properties offer significant potential for hydrogel utilization in tissue engineering, drug delivery, and bionanotechnology [3–7].

Hydrogels can be found in the form of macroscopic networks or confined to smaller dimensions such as microgels or nanogels. Sub-

micron-sized polymer hydrogels (nanogels  $\leq 200$  nm) have also attracted growing interest due to their size and unique surface properties that enable further chemical reactions and multivalent bioconjugation [8–10]. Further, nanogels may entrap drugs and biomolecules and consequently, can be highly useful for protein and gene delivery [11,12]. Recently, the development of hybrid hydrogels with nanosized inorganic clays, carbon nanotubes, and polyaniline nanosticks has been of increasing interest in the field of materials science [10]. The combination of a macroscopic hydrogel and nanogels can offer a robust solution to contemporary biomedical challenges. For example, current therapies to generate tissues (e.g. bone, nerve, and blood vessels) rely on the delivery of a single growth factor; however, typically multiple growth factors are needed to promote the complex cascade of events for tissue regeneration [13]. Nanostructured hydrogels with a biodegradable

\* Corresponding author. 4400 Fifth Avenue, Pittsburgh, PA 15213, USA. Tel.: +1 412 268 3209.

E-mail address: [km3b@andrew.cmu.edu](mailto:km3b@andrew.cmu.edu) (K. Matyjaszewski).

macroscopic network can be used as an artificial ECM for tissue regeneration and as a delivery system for the controlled release of multiple biomolecules.

Hydrogels have been used for sustained delivery of active compounds. Hydrogels have porosity due to the network structure of the cross-linked polymer chains, which allows molecular diffusion. Small molecules (e.g. peptides, proteins) can diffuse in and out of the matrix, whereas larger molecules (e.g. plasmid DNA) are often entrapped within the pores and maintained within the network only to be released as a result of matrix degradation.

The fabrication of scaffolds from natural materials, such as polysaccharides (e.g. hyaluronic acid, HA) can provide intrinsic signals within the structure that can enhance tissue formation. HA is a naturally occurring polymer, and is bioactive, non-cytotoxic, and degradable enzymatically [14–20]. Leach et al. reported that HA-based-hydrogels have large pore sizes ( $\geq 539$  nm), which may be suitable for the encapsulation of large molecules, such as plasmid DNA. However, these systems may cause rapid and uncontrolled release of relatively small molecular entities, such as peptides, proteins, and drugs. In order to control and target the release of these small compounds from HA-based scaffold, a second nano-scaled polymeric system impermeable to low molecular weight therapeutic molecules can be grafted to the macroscopic HA matrix.

In this study, we report on the synthesis of nanostructured hybrid hydrogels prepared by a combination of ATRP and FRP [21–23]. As described previously, well-defined POEO<sub>300</sub>MA nanogels can be prepared by inverse miniemulsion AGET ATRP at ambient temperature (30 °C) [24–27]. Oligo (ethylene oxide) monomethyl ether methacrylate (OEO<sub>300</sub>MA) was used as a monomer, poly (ethylene oxide) dimethacrylates (PEODM) as a cross-linker, hydroxyl-containing water-soluble ATRP as an initiator (oligo (ethylene oxide)-functionalized bromoisobutyrate, HO–EO–Br) in order to produce functional nanogels with the capacity for further chemical modifications. Fluorescent dyes were entrapped in the nanogels for labeling and as a model of encapsulation of relatively low molecular weight model substances.

Moreover, the nanogels were chemically modified to generate photoreactive and cleavable nanospheres. The nanostructured hybrid hydrogels were prepared by covalent incorporation of polymerizable POEO<sub>300</sub>MA nanogels into HA-glycidyl methacrylate (HAGM) macroscopic hydrogels via FRP under ultra-violet (UV) irradiation. A pure HAGM hydrogel with tunable physical properties was previously prepared in order to design a versatile biodegradable scaffold to match a number of tissue regeneration processes [28]. The stability of these nanostructured hybrid hydrogels against mechanical load was characterized based on composition and extent of nanogel content. RGD integrin-binding motif was incorporated into the cross-linked network through GRGDS-containing nanogels to support cellular adhesion with the nanostructured hybrid scaffold *in-vitro*. This nanostructured hybrid hydrogel offers compelling opportunities in tissue engineering and as a convenient drug delivery reservoir for multi-sized components, and as a regulator for targeted release of nanogels.

## 2. Experimental

### 2.1. Materials

OEO<sub>300</sub>MA (300 g/mol, EO units  $\approx$  5) was purchased from Aldrich and purified by passing through a column filled basic alumina to remove inhibitor. PEO 4 k (4000 g/mol), 2-hydroxyethyl methacrylate (HEMA), HA ( $1.6 \times 10^6$  g/mol), glycidyl methacrylate (GM), methacrylic anhydride (MAH), copper (II) bromide (CuBr<sub>2</sub>), dithioproprionic acid (DTPA), 4-dimethylaminopyridine (DMAP), *N,N'*-diisopropylcarbodiimide (DIC), triethylamine (TEA), Rhodamine B isothiocyanate–dextran (RITC–Dx, 60,000 g/mol), and fluorescein isothiocyanate–dextran (FITC–Dx, 60,000 g/mol) were purchased from Sigma–Aldrich and used as-received.

Dichloromethane was purchased from Sigma–Aldrich and dried over activated molecular sieves (4 Å) prior to use. Acryloyl-PEO-*N*-hydroxylsuccinimide (ACRL-PEO-NHS, 3400 g/mol) was purchased from Laysan Bio Inc. GRGDS peptide was purchased from Bachem Bioscience Inc. Photoinitiator Irgacure 2959 (I2959) was obtained from Ciba Specialty. Tris[(2-pyridyl)methyl]amine (TPMA) and HO–EO–Br were synthesized as described elsewhere [29,30]. All other chemicals used were of reagent grade and were used without further purification.

For *in-vitro* cell culture, C2C12 myoblast cells were obtained from American Type Culture Collection (Manassas, VA) and cultured in Dulbecco's Modified Eagle Media, purchased from Invitrogen (Carlsbad, CA), supplemented with 10% fetal bovine serum and 1% penicillin/streptomycin. Phosphate-buffered saline (PBS) was purchased from Invitrogen. Live/Dead<sup>®</sup> Viability/Cytotoxicity Kit was purchased from Molecular Probes, Inc. (Eugene, OR).

### 2.2. Measurements

High-resolution, 300 MHz proton NMR spectra were taken on a Bruker Avance 300 spectrometer. Deuterium oxide (D<sub>2</sub>O) was used as solvent, and the polymer concentrations were varied between 0.5% and 3% by mass fraction. All spectra were run at room temperature, 15 Hz sample spinning, 45° tip angle for the observation pulse, and a 10 s recycle delay, for 128 scans. The standard relative uncertainty for calculation of reaction conversion via <sup>1</sup>H NMR arises from the choice of the baseline and is estimated to be 8%.

Particle size and size distribution of nanogels were measured by dynamic light scattering (DLS) on High Performance Particle Sizer, Model HP5001 from Malvern Instruments, Ltd. Confocal imaging was performed on an Olympus FV1000 microscope. All imaging conditions, including laser power, photomultiplier tube, and offset settings, remained constant for each comparison set and at least three different random sites were probed on the samples.

### 2.3. Synthesis of PEODM

PEODM was prepared as described previously [31]. Briefly, the synthesis of PEODM 4 k is as follows. PEO 4 k (10 g, 0.0025 mol), 2.2 equiv of MAH (0.85 g, 0.0055 mol), and TEA (0.4 mL) were reacted in 30 mL of dichloromethane over freshly activated molecular sieves (6 g) for 4 days at room temperature. The solution was filtered over alumina and precipitated into ethyl ether. The product was filtered and then dried in a vacuum oven overnight at room temperature.

### 2.4. Synthesis of ACRL-PEO-GRGDS

GRGDS peptide was dissolved in anhydrous DMF containing 4 M excess of TEA. ACRL-PEO-NHS was also dissolved in anhydrous DMF and immediately mixed with 1.1 M excess of peptide. After incubating for 3 h at room temperature, ACRL-PEO-GRGDS was precipitated twice in cold anhydrous ether and dried in a vacuum oven overnight at room temperature.

### 2.5. Synthesis of HAGM

Photopolymerizable HAGM with a degree of methacrylation (DM) of 32% was prepared as reported previously [28]. 1.0 g of HA ( $1.6 \times 10^6$  g/mol) was dissolved in 200 mL phosphate buffer saline (PBS, pH  $\sim$ 7.4) and 67 mL of dimethylformamide (DMF), and subsequently mixed with 13.3 g of GM and 6.7 g of TEA. After 10 days of reaction at room temperature, the solution was precipitated twice in a large excess of acetone (20 times the volume of the reaction solution), filtered, dried in vacuum oven overnight at 50 °C, and dialyzed for 3 days against deionized H<sub>2</sub>O using dialysis membrane with molecular weight cut-off (MWCO) of 5000.

### 2.6. Synthesis of well controlled RITC–Dx or FITC–Dx-containing HO-PEO<sub>300</sub>MA nanogels by cyclohexane inverse miniemulsion AGET ATRP

FITC- or RITC-loaded POEO<sub>300</sub>MA nanogels functionalized with hydroxyl groups and GRGDS peptide were prepared by AGET ATRP of OEO<sub>300</sub>MA in the presence of HO–EO–Br in inverse miniemulsion of water/cyclohexane at ambient temperature (30 °C) using Span 80 as an oil-soluble surfactant, TPMA/CuBr<sub>2</sub> as the catalyst precursor, PEODM as the cross-linker, and ascorbic acid (AsCA) as a reducing agent. FITC–Dx (60,000 g/mol) or RITC–Dx (60,000 g/mol) was used to tag the nanogels.

The synthesis of POEO<sub>300</sub>MA nanogels by inverse miniemulsion ATRP in cyclohexane was carried out according to the following ratio: [OEO<sub>300</sub>MA]<sub>0</sub>/[HO–EO–Br]<sub>0</sub>/[CuBr<sub>2</sub>/TPMA]<sub>0</sub>/[AsCA]<sub>0</sub>/[PEODM]<sub>0</sub>/[FITC–Dx/RITC–Dx]<sub>0</sub> = 150/1/0.5/0.45/4/0.02. GRGDS-PEO<sub>300</sub>MA nanogels were prepared in the same manner using ACRL-PEO-GRGDS as a comonomer at a final concentration of 1.3 mM (low peptide content) or 6.5 mM (high peptide content).

A typical procedure for the synthesis is described below. OEO<sub>300</sub>MA (2 g, 6.67 mmol), HO–EO–Br (13.8 mg, 0.044 mmol), PEODM (711 mg, 0.178 mmol), TPMA (6.5 mg, 0.022 mmol), CuBr<sub>2</sub> (5 mg, 0.022 mmol), FITC–Dx or RITC–Dx (60 mg, 0.001 mmol), ACRL-PEO-GRGDS (20 mg or 100 mg, 0.0026 mmol or 0.0065 mmol, respectively) and water (2 mL) were mixed in a 50 mL round bottomed flask

at room temperature. The resulting clear solution was mixed with a solution of Span 80 (1.42 g) in cyclohexane (28.5 g), and the mixture was sonicated for 2 min in an ice bath at 0 °C to form a stable inverse miniemulsion. The dispersion was transferred into a 50 mL Schlenk flask, and then bubbled with argon for 30 min. The flask was immersed in an oil bath preheated to 30 °C, and then an argon-purged aqueous solution of AscA (3.5 mg, 0.02 mmol) was added via syringe to activate the catalyst and start the polymerization. The polymerization was stopped after 4 h by exposing the reaction mixture to air. After synthesis, the nanogels were separated by centrifugation, suspended in water, and dialyzed against deionized water for 2 days using dialysis membrane with MWCO of 13,000.

## 2.7. Methacrylation of HO-POEO<sub>300</sub>MA nanogels

### 2.7.1. Methacrylation of HO-POEO<sub>300</sub>MA nanogels (MA-nanogels) with MA

Polymerizable MA-POEO<sub>300</sub>MA nanogels were prepared in one step by reaction of HO-containing-nanogels with methacrylic anhydride. HO-containing nanogels (500 mg, HO-groups ≈ 27 μmol) were swollen in 5 mL of DMF for 3 h. A solution of MAH (250 mg, 1.6 mmol) and TEA (30 mg, 0.3 mmol) in 5 mL of DMF was added upon stirring. The reaction was allowed to proceed overnight. The solvent was removed by evaporation under a stream of air for 6 h and the modified-nanogels were dried under vacuum at RT overnight. The nanogels were subsequently swollen in water and dialyzed against distilled water for 2 days using dialysis membrane with MWCO of 10,000.

### 2.7.2. Methacrylation of HO-POEO<sub>300</sub>MA nanogels (MA-S<sub>2</sub>-nanogels) with DTPA/HEMA

MA-S<sub>2</sub>-POEO<sub>300</sub>MA nanogels were prepared by coupling hydroxyl-containing nanogels with DTPA and subsequently methacrylated with HEMA. Briefly, HO-containing-nanogels (375 mg, HO-groups ≈ 20 μmol) were swollen in 10 mL of DMF. A total of (0.2 g) of DMAP, (0.25 g, 2 mmol) DIC and (2 g, 10 mmol) of DTPA was added and the reaction mixture was allowed to proceed for 1 day at RT. The nanogels were centrifuged and washed twice with DMF/methanol (70:30). DTPA-nanogels (375 mg, 20 μmol) were swelled in 10 mL of DMF. A total of (0.2 g) of DMAP, (1 g, 8 mmol) DIC and (2 g, 16 mmol) of HEMA were added to the flask upon stirring, and the reaction mixture was allowed to proceed for 1 day at RT. The nanogels were centrifuged and washed again with DMF/methanol (70:30) and dried at RT. The nanogels were subsequently swollen back in water and dialyzed against distilled water for 2 days using dialysis membrane with MWCO of 10,000.

## 2.8. Preparation and characterization of nanostructured hybrid hydrogels by FRP

### 2.8.1. Preparation of nanostructured hybrid hydrogels

The macromonomer solution was prepared by mixing 5% (wt/v) HAGM and MA-nanogels or MA-S<sub>2</sub>-nanogels at various mass fractions (0, 1, 5, and 10% wt/v) with deionized H<sub>2</sub>O in the presence of photoinitiator (I2959, 0.1% by mass fraction). Disc-shaped samples were cured with a long wavelength UV source (365 nm, 300 μW/cm<sup>2</sup>) for 10 min to obtain chemically cross-linked hydrogels.

### 2.8.2. Characterization of vinyl group conversion of nanostructured hybrid hydrogels by <sup>1</sup>H NMR

The macromonomer solution was prepared by mixing 5% (wt/v) HAGM and 1% (wt/v) MA-nanogels with D<sub>2</sub>O in the presence of photoinitiator (I2959, 0.1% by mass fraction). 1 mL of the macromonomer solution was transferred and sealed in an NMR tube before being cured under a UV source (365 nm, 300 μW/cm<sup>2</sup>) for 10 min to form a cross-linked hydrogel. <sup>1</sup>H NMR spectroscopy was used to characterize conversion of vinyl groups in the gels. The conversion was evaluated from the comparison of the relative peak intensity of the methylene protons from MA-nanogels and HAGM to the benzyl peaks from the photoinitiator compound.

## 2.9. Release of nanogels from 3D hydrogel by reduction of disulfide bonds

Fluorescence spectroscopy was used to detect RITC-Dx or FITC-Dx-labeled nanogels in the matrix. The presence of labeled nanogels in the macroscopic hydrogels was detected by the luminescence produced by Rhodamine B or fluorescein using a Tecan Spectra Fluor (Tecan US). Nanogel release from nanostructured HAGM-co-MA-S<sub>2</sub>-nanogels hybrid hydrogel was investigated at RT under different concentrations of glutathione (1, 5, and 10% wt/v) and at different incubation time (0, 24, and 48 h). The absorbance value of each sample at different incubation times was read at 490 nm with a microplate reader. Wells containing no gel and pure HAGM were used as blank control and background, respectively.

## 2.10. Swelling and mechanical testing

To determine the effect of nanogels on the nanostructured hybrid hydrogel properties, the swelling ratio and mechanical properties of each sample were measured.

### 2.10.1. Swelling measurements

Hydrogel disks in triplicate were prepared by photopolymerization in phosphate-buffered saline solution (PBS, pH ~7.4). The equilibrium mass swelling ratio ( $Q_M$ ) was calculated by the following equation (1):

$$Q_M(\%) = [m_s/m_d \times 100] \quad (1)$$

where  $m_s$  and  $m_d$  were fully swollen gel and dried gel weights, respectively. The swelling data were corrected for the PBS by subtracting the soluble fraction of salt from the gel.

### 2.10.2. Mechanical testing

Uniaxial compression measurements were used on nanostructured hybrid hydrogels to assess mechanical strength. Shear modulus was determined using uniaxial compression measurements performed by a TA.XT21 HR texture analyzer (Stable Micro Systems, UK). This apparatus measures the deformation ( $\pm 0.001$  mm) as a function of an applied force ( $\pm 0.01$  N). Cylindrical hydrogels (height = diameter = 5 mm) were deformed (at constant volume) between two parallel glass plates. Shear modulus ( $G$ ) was calculated from nominal stress,  $\sigma$  (force divided by undeformed cross-sectional area), using equation (2) [32]:

$$\sigma = G(A - A^{-2}) \quad (2)$$

where  $A$  is the macroscopic deformation ratio ( $A = L/L_0$ ,  $L$  and  $L_0$  are the lengths of the deformed and undeformed specimen, respectively). Measurements were carried out in triplicate at deformation ratios  $0.7 < A < 1$ . No volume changes or barrel distortions were detected.

## 2.11. In-vitro biocompatibility and cell response evaluation of nanostructured GRGDS-POEO<sub>300</sub>MA nanogels/HAGM hybrid hydrogels

After photopolymerization, the gels were placed in the bottom of a 24-well plate. The gels were subsequently washed two times in sterile PBS, sterilized once in 70% ethanol and washed twice with sterile PBS, and finally conditioned in cell culture medium. Mouse muscle myoblast C2C12 cell lines were seeded onto the hydrogel disks at a density of 50,000 cells/gel. The cells were cultured for 4 days to assess cytotoxicity. The Live/Dead<sup>®</sup> Viability/Cytotoxicity Kit contains Calcein AM to measure intracellular esterase activity. Live cells fluoresce green at 494–518 nm, while Ethidium homodimer 1 enters cells with a damaged plasma membrane and fluoresces bright red at 528–617 nm. For live dead staining, the cell culture media was aspirated and the wells rinsed with PBS, and the cells were incubated in the dark for 30 min at 37 °C with live/dead stain (Calcein 1:2000 and Ethidium homodimer 1:500 diluted in PBS). After incubation, the cells were observed with a fluorescent microscope (Zeiss Axiovert 200 microscope) and the images were captured using a monochrome CCD camera and pseudocolored.

## 3. Results and discussion

### 3.1. Synthesis and characterization of nanostructured hybrid hydrogels

Well-controlled fluorescent dye-labeled nanogels were successfully prepared by AGET ATRP of OEO<sub>300</sub>MA in inverse miniemulsion of water/cyclohexane at ambient temperature. Hydroxyl-containing ATRP initiator was used in the controlled radical polymerization in order to produce functional HO-POEO<sub>300</sub>MA nanogels with the capability to be successively functionalized. Cell-adhesive nanogels were synthesized using ACRL-PEO-GRGDS as a comonomer during the polymerization. RGD integrin-binding motif was used to promote cell–substrate interactions.

As shown in Fig. 1, GRGDS functionalized POEO<sub>300</sub>MA nanogels loaded with fluorescent dye (Rhodamine B or fluorescein) were prepared by AGET ATRP. ATRP offers the advantage to prepare nanogels with controllable diameter and functionalities. The particle size was examined by DLS at 20 °C (swollen state) and the hydrodynamic diameter of the nanogels was estimated to be  $120 \pm 8$  nm and  $111 \pm 7$  nm for RITC-Dx-loaded and FITC-loaded POEO<sub>300</sub>MA nanogels, respectively.

A set of nanogels with pendant hydroxyl-moieties was modified with methacrylic anhydride with the aim to functionalize the particle surface with photopolymerizable groups (MA-nanogels). As shown in Fig. 2, the methacrylation of the nanogels was confirmed by <sup>1</sup>H NMR. The two main sets of peaks at 5.70–

5.90 ppm and 6.10–6.30 ppm (a and b, respectively) represent the vinyl methylene protons from pendant methacrylated moieties.

In order to prepare cleavable nanogels, MA- $S_2$ -nanogels based on pendant methacrylate groups with disulfide moieties were prepared by reaction of hydroxyl-containing nanogels with DTPA followed by reaction with HEMA using DIC/4-DMAP coupling chemistry. The functionalization of nanogels was confirmed by  $^1\text{H}$  NMR. As shown in Fig. 3, the chemical shifts at 6.10, 5.66, 2.70, 2.55,

and 1.86 ppm (a, b, c, d, and e, respectively) confirm successful modification of nanogels with disulfide linkers conjugated with methacrylated groups.

The photopolymerization of HAGM or PEODM along with MA-nanogels resulted in the formation of a stable macroscopic scaffold hybridized with nanogels. In contrast, the photopolymerization of HAGM with MA- $S_2$ -nanogels resulted in a scaffold with cleavable nanogels. In the presence of glutathione, the disulfide bridges can

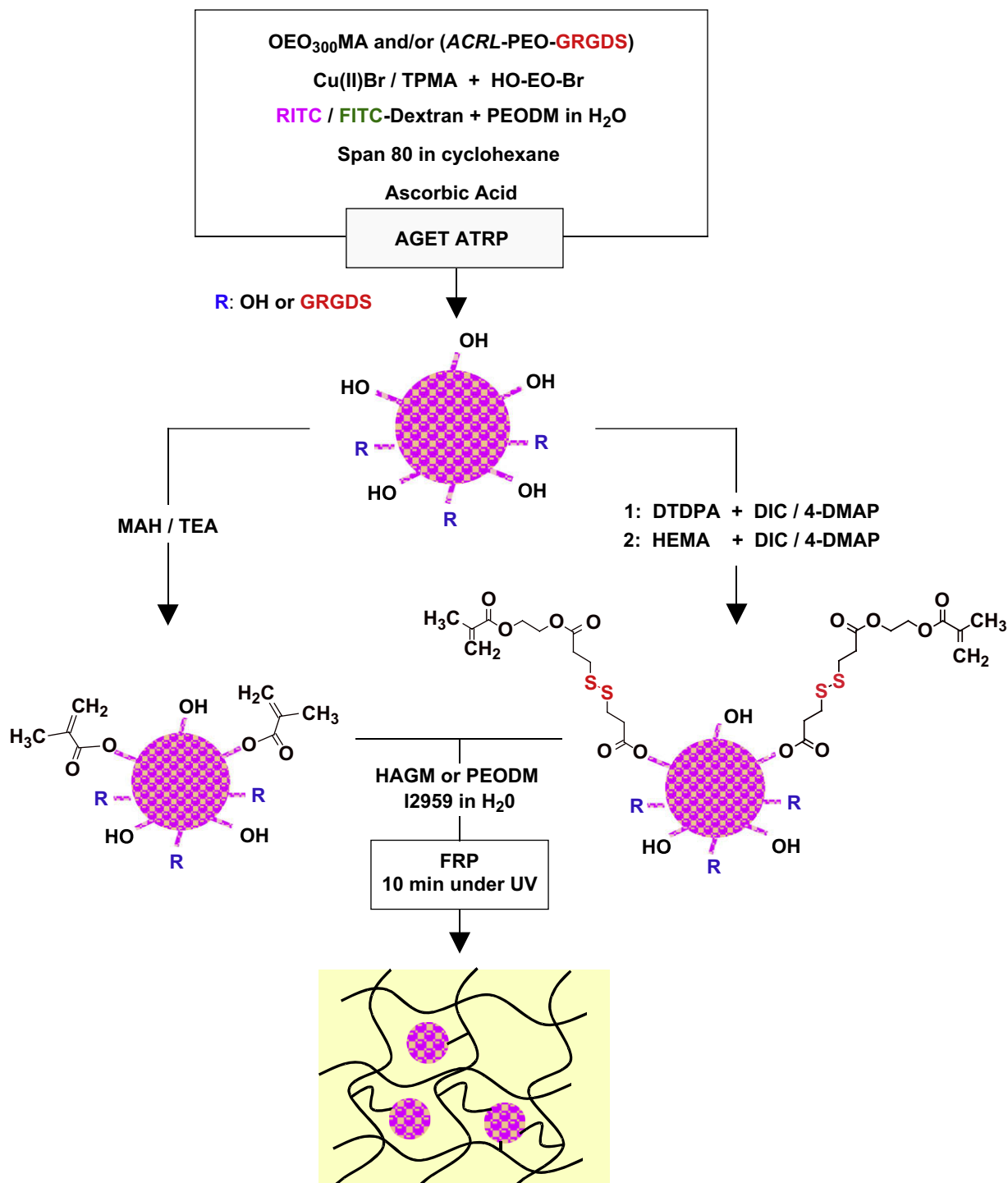


**Fig. 1.** Synthesis of well-defined fluorescent dye-loaded GRGDS-POEO<sub>300</sub>MA nanogels by AGET ATRP in inverse miniemulsion of water/cyclohexane at ambient temperature. The nanogels were subsequently substituted with MAH or coupled with DTPA/HEMA to incorporate cleavable photopolymerizable groups. Nanostructured hybrid hydrogels were prepared by covalent incorporation of methacrylated POEO<sub>300</sub>MA nanogels into macroscopic HAGM or PEODM hydrogels via FRP under ultra-violet (UV) irradiation.

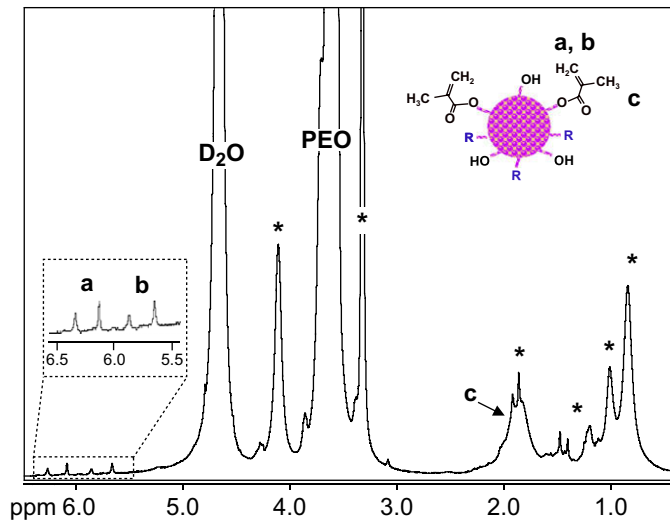


**Fig. 2.**  $^1\text{H}$  NMR spectra of methacrylated POEO<sub>300</sub>MA nanogels (MA-nanogels). Two main sets of peaks at 5.70–5.90 ppm and 6.10–6.30 ppm (a and b, respectively) confirmed chemical modification of hydroxyl-containing nanogels with methacrylated moieties. Characteristic chemical shifts from peptide (GRGDS) are represented with the symbol \*.

be easily reductively cleaved, leading to dissociation of FITC-nanogels-S<sub>2</sub>-HA into FITC-nanogels-SH and thiolated HA [29].

$^1\text{H}$  NMR spectroscopy was used to monitor vinyl conversion and cross-linking efficiency of HAGM and polymerizable nanogels. As shown in Fig. 4, the methacrylated nanogels were efficiently photo-attached to the scaffold, as a high vinyl group conversion was achieved within 10 min of UV irradiation, suggesting nearly complete reaction. The conversion was evaluated by comparing the relative peak intensity of the methylene protons from MA-nanogels (●) and HAGM ◆ and benzyl peaks from the photoinitiator used as reference (\*).

To complement  $^1\text{H}$  NMR spectroscopy, confocal laser microscopy was employed to image fluorescent dye-loaded nanogels inside the hydrogels. As shown in Fig. 5, FITC-Dx-labeled nanogels

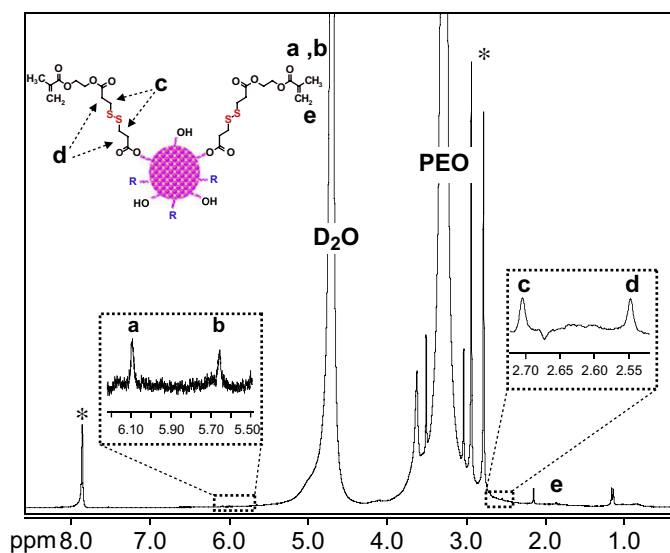


**Fig. 3.**  $^1\text{H}$  NMR spectra of reductive methacrylated POEO<sub>300</sub>MA nanogels (MA-S<sub>2</sub>-nanogels). Chemical shifts at 6.10 ppm, 5.66 ppm, 2.70 ppm, 2.55 ppm, and 1.86 ppm (a, b, c, d, and e, respectively) confirmed conjugation of hydroxyl-containing nanogels with cleavable disulfide methacrylated groups. Impurity peaks from solvent (DMF) are represented with the symbol \*.

(red spots) are dispersed in the scaffold stained with FITC (green clusters). However, the clusters of nanogels are presumably due to pre-aggregation of nanogels before photopolymerization.

### 3.2. Physical properties of nanostructured hybrid hydrogels

The swelling behavior of a series of nanostructured 5% (wt/v) HAGM hydrogels with a broad range of nanogel content (0–10% wt/v) was investigated (Fig. 6). The hybridized gels exhibit at equilibrium a lower degree of swelling than pure HAGM gel.

The incorporation of nanogels from 0 to 10% (wt/v) into the hydrogels led to a gradual decrease of swelling. However, as shown in Fig. 6, at low concentration (1%), the nanogels have minimal impact on gel swelling properties. In contrast, at higher concentration, the nanogel content has a greater impact on the swelling ratio, with 22.16 and 21.13 vs. 30.36, for 5% and 10% vs. 0% (wt/v) nanogels, respectively. This behavior is expected since the incorporation of nanogel particles increases the total solid content of the hydrogel (in equation (1)  $m_d$  is increased).

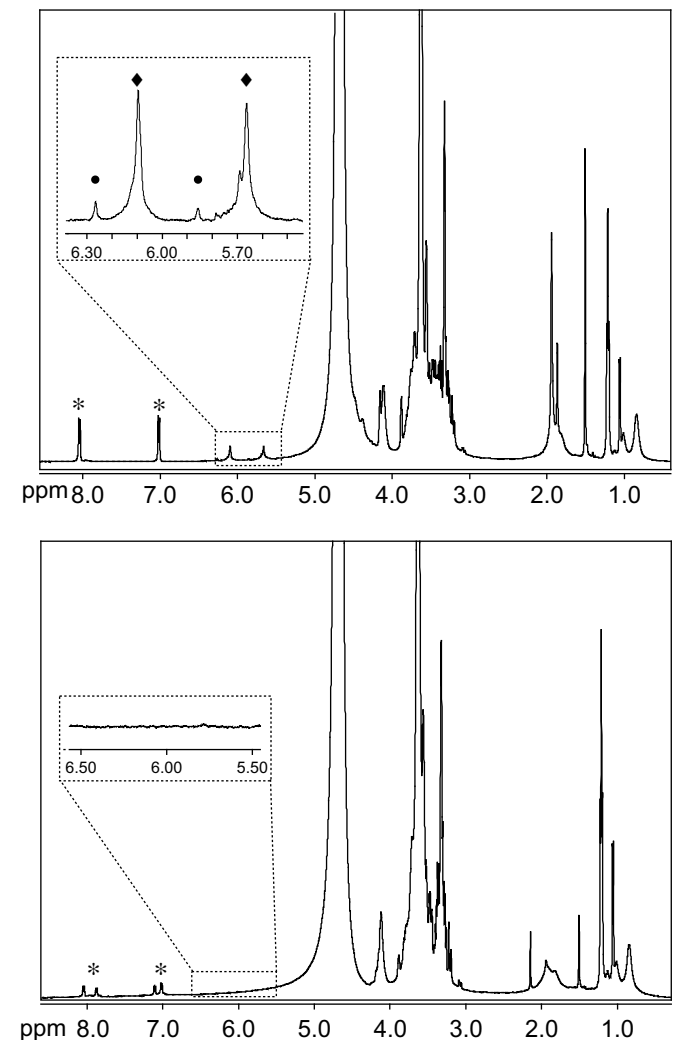


**Fig. 4.**  $^1\text{H}$  NMR of uncross-linked (top) and cross-linked (bottom) nanostructured HAGM-co-MA-nanogels hybrid hydrogel in D<sub>2</sub>O. Photopolymerization is induced directly in an NMR tube. After photocross-linking, the methacrylate peaks (● and ◆) from methacrylated nanogels and HAGM, respectively, disappeared after 10 min irradiation under a long wavelength UV source (365 nm, 300  $\mu\text{W}/\text{cm}^2$ ). The conversion was evaluated from the comparison of the relative peak intensity of the methylene protons from MA-nanogels and HAGM to the benzyl peaks from the photoinitiator (I2959) represented with the symbol \*.

The mechanical characteristics of the scaffolds can be used to understand properties of the nanostructured hydrogels. The shear moduli ( $G$ ) of the hybrid hydrogels were measured by uniaxial compression and calculated using equations derived from the strain energy function.

Fig. 7 shows nominal stress  $\sigma$  as a function of the deformation ratio  $\Lambda$  for 5% (wt/v) HAGM (DM 32%) with various concentrations of nanogels. The insets of Fig. 7 plot normal stress vs. deformation ratio according to the Mooney–Rivlin representation equation (3) [33]:

$$\sigma = 2(\Lambda - \Lambda^{-2})(C_1 + C_2/\Lambda) \quad (3)$$

where  $C_1$  and  $C_2$  are constants. It is apparent that the value of  $C_2$  is approximately zero. This result is consistent with many previous findings reported for highly swollen polymer networks. The shear moduli of hybrid HAGM gels prepared with various MA-nanogel fractions (0, 1, 5, and 10% wt/v) were evaluated to understand the relationship between nanostructure and gel properties. No significant differences were observed between the samples. As seen in Fig. 8, uniaxial compression test indicated that 5% (wt/v) hybrid HAGM hydrogels were mechanically robust and had minimal shear moduli variation between 35.6 kPa and 37.8 kPa regardless of the nanogel content. Clearly, the hybrid gels had mechanical properties similar to pure HAGM hydrogel, which is likely to be due to comparable cross-link density. Furthermore, the present results imply that no significant interaction exists between the nanogels and the polymeric network. Apparently, the nanogel particles behave like “solvent” molecules, i.e., they replace a certain amount of solvent without modifying the elastic response of the gels. Therefore, it is expected that at higher nanogel content, the swelling ratio will be lower since the covalently incorporated nanospheres occupy a significant volume fraction of HAGM gels. This picture is consistent with the observed swelling behavior of

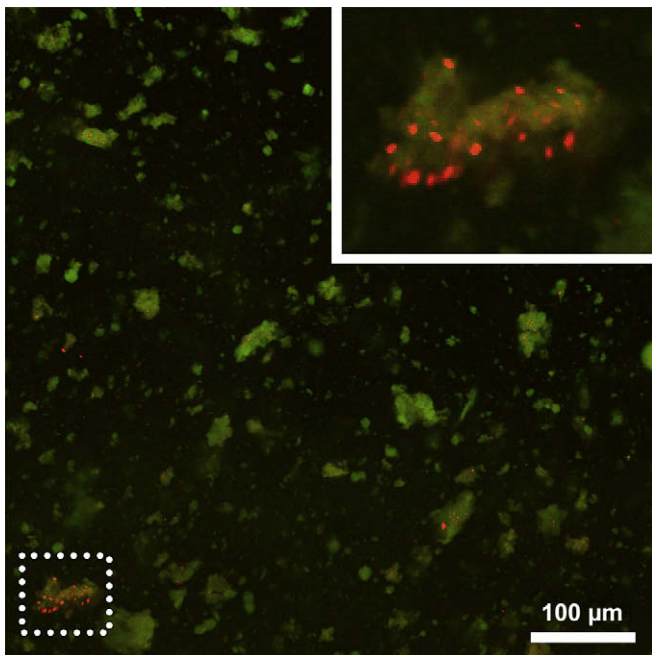


Fig. 5. Confocal microscopy image of nanostructured PEODM-co-MA-nanogels hybrid hydrogel after 1 day of incubation in PBS. RITC-Dx-labeled nanogels (1% wt/v, red spots) are covalently dispersed in the scaffold stained with FITC (10% wt/v, green clusters).

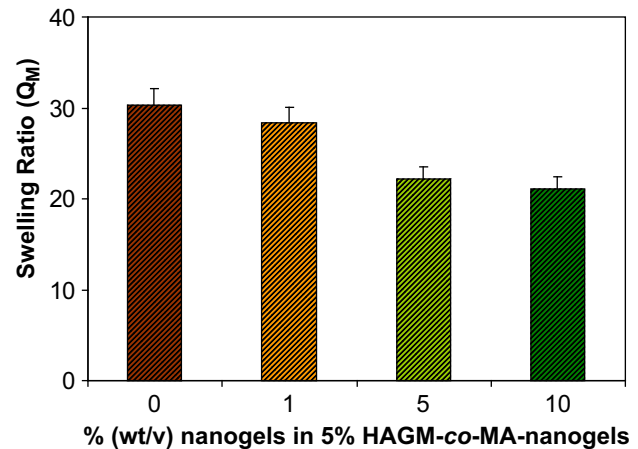


Fig. 6. Swelling ratio ( $Q_M$ ) of a set of nanostructured 5% (wt/v) HAGM hybrid hydrogel with various nanogel contents (0, 1, 5, and 10% wt/v).

the hybrid gels where  $Q_M$  decreased when the nanogel content increased from 1 to 10% (wt/v).

The rheological measurements also indicate that the mechanical integrity of nanostructured HAGM hydrogels was preserved, as their shear moduli were close to that of the pure HAGM hydrogel. The incorporation of nanogels into the scaffold is expected to have an impact on swelling and mechanical properties. However, variation of shear modulus is less pronounced than is seen in the swelling ratio. These characteristics can be useful in a quick approximation of hybrid gel properties where the stability and mechanical integrity of nanostructured hydrogels are similar to pure HAGM gel itself.

### 3.3. Controlled release of nanogels from 3D hybrid hydrogels

In this section we investigate the effect of covalent attachment of the nanogel particles on their transport properties in the swollen network. To this end we used labeled nanogels imbedded in the gel matrix. Fluorescent dye-labeled nanogels incorporated to the macroscopic hydrogels were detected by the luminiscence produced by Rhodamine or fluorescein. As shown in Fig. 9, for encapsulated nanogels (uncross-linked), absorbance decreased dramatically within 2 h of incubation in PBS and nearly completely

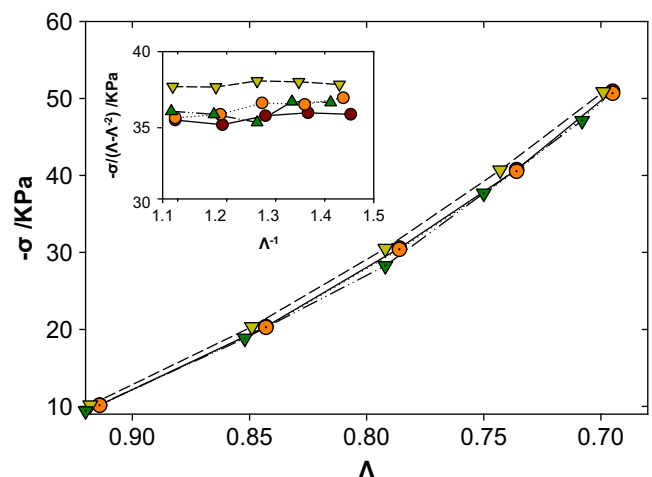
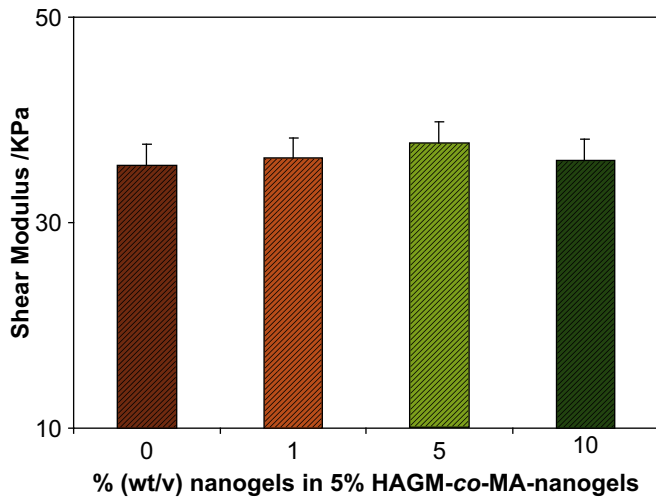


Fig. 7. Nominal stress ( $\sigma$ ) measured as a function of the deformation ratio ( $\Lambda$ ) for nanostructured 5% (wt/v) HAGM hybrid hydrogels with 0% (●), 1% (○), 5% (▼), and 10% (▽) MA-nanogels. The insets show the Mooney–Rivlin representation plotting the reduced stress vs.  $1/\Lambda$ . Note that the  $\sigma$  is negative due to the compressive forces used.



**Fig. 8.** Influence of gel hybridization on the mechanical properties. Shear modulus of nanostructured 5% (wt/v) HAGM hybrid hydrogels was measured at various mass fractions (wt/v) of MA-nanogels (0, 1, 5, and 10% wt/v).

leached after 1 day. This observation suggests matrix permeability toward nanosized particles, allowing nanogels to diffuse out of the scaffold. The uncontrolled release of nanogels can be prevented through covalent immobilization. Our approach was to photocross-link polymerizable nanogels with HAGM. As observed in Fig. 9, covalent attachment clearly decreased release of nanogels. For the nanostructured hybrid hydrogels, absorbance decreased within 1 day, presumably due to gel swelling and partial release of unreacted nanogels, followed by a constant absorbance independently of time. This confirms the covalent binding of nanogels into the matrix, leading to the formation of a stable nanostructured HA-based hybrid gel. These nanogels are permanently incorporated into the network unless the macroscopic matrix is degraded enzymatically by hyaluronidase.

Thus, hybrid gels with cleavable disulfide bridges (HAGM-co-MA-S<sub>2</sub>-nanogels) were prepared to control the release of anchored nanogels through disulfide bond dissociation without matrix degradation. The covalent incorporation and controlled release of

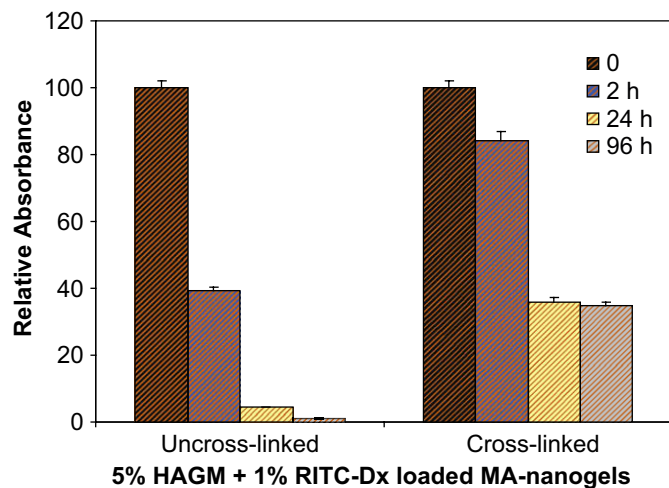


**Fig. 9.** Absorbance of encapsulated 1% (wt/v) RITC-Dx-labeled nanogels (uncross-linked) and photocross-linked 1% (wt/v) RITC-Dx-labeled MA-nanogels (cross-linked) in macroscopic 5% (wt/v) HAGM hydrogel. The nanostructured hybrid hydrogels were incubated in PBS and the absorbance was recorded at different time points (0, 2, 24, and 96 h).

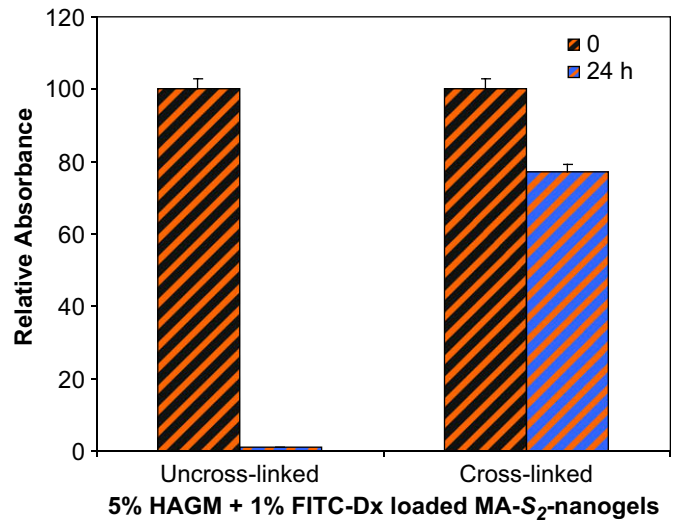


**Fig. 10.** Absorbance of encapsulated 1% (wt/v) FITC-Dx-labeled nanogels (uncross-linked) and photocross-linked 1% (wt/v) FITC-Dx-labeled MA-S<sub>2</sub>-nanogels (cross-linked) in macroscopic 5% (wt/v) HAGM hydrogel. The nanostructured hybrid hydrogels were incubated in PBS and the absorbance was recorded at two time points (0 and 24 h). After 1 day of incubation, a constant absorbance for HAGM-co-MA-S<sub>2</sub>-nanogels hybrid hydrogels was recorded independently of time.

nanogels from the matrix under a reducing environment was evaluated by fluorescence spectroscopy. As observed with MA-nanogels, similar trends for the covalent attachment of MA-S<sub>2</sub>-nanogels to the scaffold were observed (Fig. 10). When incubated in PBS, the absorbance signal decreased slightly within 1 day and remained constant independently of time. This confirms that the nanogels are covalently incorporated into the network and cannot diffuse out unless reductive cleavage of disulfide bonds alternatively to enzymatic matrix degradation.

The controlled release studies were conducted after the hybrid gels had reached equilibrium size. Glutathione was chosen as a non-enzymatic reducing agent, since it is a naturally derived tripeptide and one of the major cellular reducing agent. The incubation of hybrid hydrogels in solutions with glutathione showed progressive decrease of absorbance values suggesting controlled release of nanogels from the scaffold (Fig. 11). The cleavage of

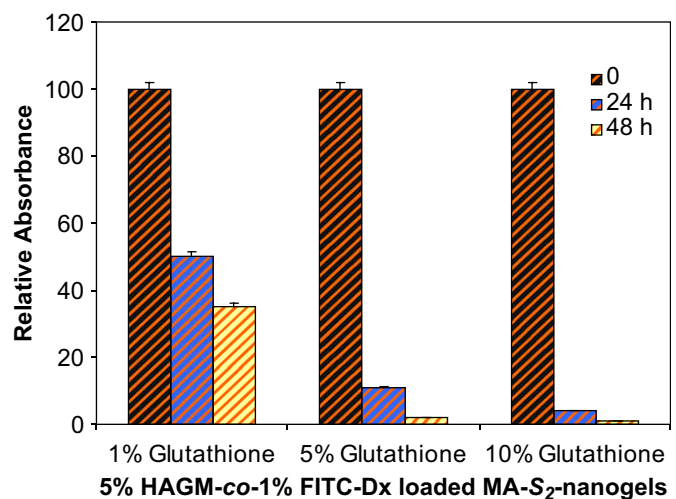


**Fig. 11.** Disulfide bonds reduction and controlled release of 1% (wt/v) FITC-Dx-labeled nanogels from nanostructured 5% (wt/v) HAGM-co-MA-S<sub>2</sub>-nanogels hybrid hydrogel. Nanogel release was investigated at RT under different concentrations of glutathione (1, 5, and 10% wt/v) and at different incubation time points (0, 24, and 48 h).

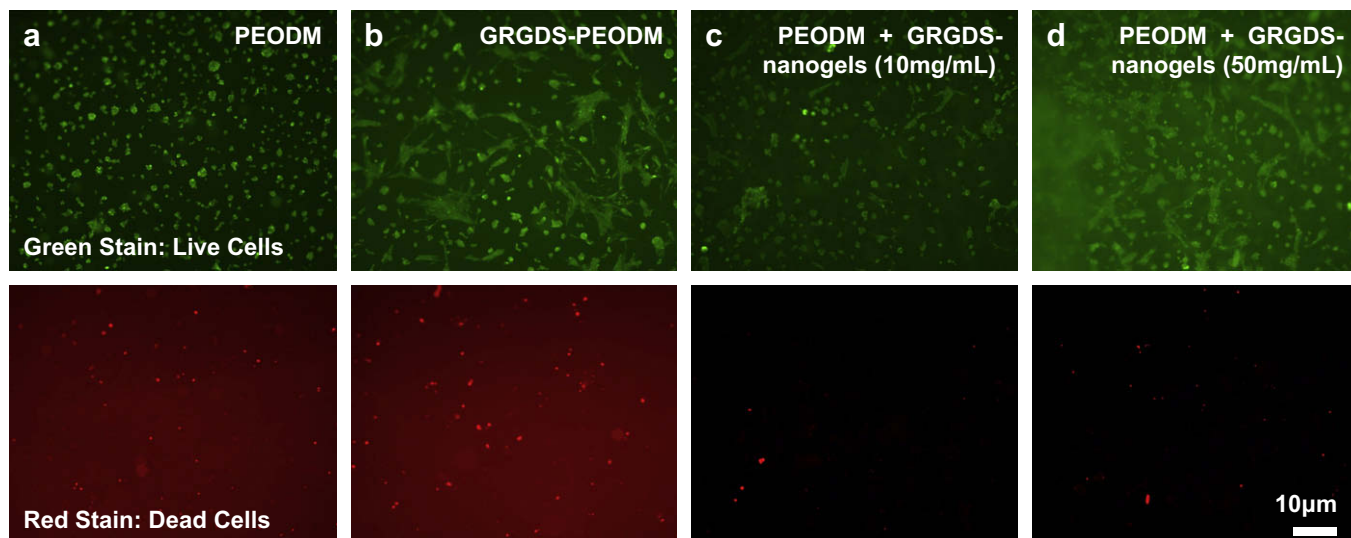


**Fig. 12.** Mouse myoblast cells (C2C12) seeded on a series of 10% (wt/v) hydrogels; PEODM (a), GRGDS-modified PEODM (b), PEODM-co-GRGDS-MA-nanogels (nanogel content: 10 mg/mL) (c), and PEODM-co-GRGDS-MA-nanogels (nanogel content: 50 mg/mL) (d). The cells were cultured for 4 days and stained with the live stain on top (green) and dead cell stain on the bottom (red).

disulfide bonds and the redox equilibrium of thiol/disulfide are strongly related to the levels of glutathione used. At lower glutathione concentrations (1% wt/v) the nanogels are dissociated more slowly than at higher concentrations (5 and 10% wt/v). At these high concentrations of reducing agent, approximately 90% of nanogels were released within 1 day, reaching nearly 100% release after 2 days. In contrast, at the lowest concentration, more than 35% of nanogels were still covalently attached to the HAGM network after 2 days.

#### 3.4. Biocompatibility and cell adhesiveness of GRGDS-containing nanostructured hybrid hydrogels

In order to assess cytotoxicity and cell adhesion, GRGDS functionalized MA-nanogels were covalently incorporated into PEODM scaffolds. Two concentrations of GRGDS-containing nanogels were studied (10 and 50 mg/mL) to evaluate the optimal peptide concentration required for cell–substrate interactions. To test cell viability and attachment, 50,000 C2C12 myoblasts/gel were cultured for 4 days. Cell viability was assessed using live dead staining as shown in Fig. 12.

The data suggest that nanostructured gels based on PEODM-co-GRGDS-nanogels are non-cytotoxic ( $\geq 95\%$  cell viability) and support cell attachment. At low nanogel concentration (10 mg/mL) (Fig. 12c), a moderate cell adhesion to the scaffold was observed when compared to unmodified PEODM hydrogel (Fig. 12a). However, increasing GRGDS-nanogel concentration to 50 mg/mL promoted better adhesion and spreading of cells (Fig. 12d). In fact, at this concentration adhesion and spreading were comparable to GRGDS-modified PEODM hydrogel (Fig. 12b), which was used as our positive control. This observation insinuates that cells were not sensitive to variations in molecular architecture and were able to recognize the integrin-binding motif regardless of the peptide localization, GRGDS grafted to nanogels or to a macroscopic scaffold.

#### 4. Conclusion

Nanostructured hybrid hydrogels were successfully synthesized by a combination of ATRP and FRP. Well-defined POEO<sub>300</sub>MA

nanogels were prepared by AGET ATRP and subsequently functionalized with methacrylate moieties. Polymerizable nanogels were covalently incorporated into a 3D matrix via photopolymerization. The nanostructured hybrid hydrogels exhibited rapid gelation under mild conditions with nearly complete conversion after 10 min irradiation under UV. The introduction of disulfide moieties into the polymerizable groups resulted in releasable nanogels from the cross-linked network under reduction. Hybridization of HAGM hydrogels with photopolymerizable nanogels had a minimal effect on the shear modulus, suggesting mechanical integrity of gels was conserved while the swelling ratio decreased with increased nanogel mass fraction. The nanogels seem to behave like “solvent” molecules without significantly affecting the elastic response of the gels. *In-vitro* assays suggest that these nanostructured hybrid hydrogels are cytocompatible and the introduction of GRGDS into the nanogel structure promoted cell attachment within 4 days of incubation. Consequently, these nanostructured hybrid scaffolds with cleavable nanogels seem promising for tissue engineering applications enabling control over release of sequential encapsulated biomolecules, such as multiple growth factors required at distinct stages in the development of important regenerative processes in biology and medicine.

#### Acknowledgements

The authors gratefully acknowledge Professor Simon Watkins (Center for Biologic Imaging, University of Pittsburgh School of Medicine) for access to the confocal microscope and Glenn Papworth operating the confocal microscope. Financial support was provided from NIDCR DE R01-15392-4 (JOH), NSF DMR 05-43953, and from U.S. Army DAMD 17-02-1-0717 (NRW).

#### Appendix

Figures with essential colour discrimination. Certain figures in this article, in particular Figs. 1–3, 5 and 12, are difficult to interpret in black and white. The full colour images can be found in the online version, at doi:10.1016/j.biomaterials.2009.06.011.

## References

- [1] Byrne ME, Park K, Peppas NA. Molecular imprinting within hydrogels. *Adv Drug Deliv Rev* 2002;54:149–61.
- [2] Kopecek J. Polymer chemistry: swell gels. *Nature* 2002;417:388–91.
- [3] Brandl F, Sommer F, Goeperich A. Rational design of hydrogels for tissue engineering: impact of physical factors on cell behavior. *Biomaterials* 2007;28:134–46.
- [4] Hoffman AS. Applications of thermally reversible polymers and hydrogels in therapeutics and diagnostics. *J Control Release* 1987;6:297–305.
- [5] Langer R. Drug delivery. *Drugs on target*. Science 2001;293:58–9.
- [6] Langer R, Vacanti JP. Tissue engineering. *Science* 1993;260:920–6.
- [7] (a) Peppas NA, Hilt JZ, Khademhosseini A, Langer R. Hydrogels in biology and medicine: from molecular principles to bionanotechnology. *Adv Mater* 2006;18:1345–60;  
(b) Rapoport N. Physical stimuli-responsive polymeric micelles for anti-cancer drug delivery. *Progr Polym Sci* 2007;32:962–90;  
(c) Kabanov AV, Gendelman HE. Nanomedicine in the diagnosis and therapy of neurodegenerative disorders. *Progr Polym Sci* 2007;32:1054–82;  
(d) Lutz JF, Boerner HG. Modern trends in polymer bioconjugates design. *Progr Polym Sci* 2008;33:1–39.
- [8] Das M, Mardiyani S, Chan WCW, Kumacheva E. Biofunctionalized pH-responsive microgels for cancer cell targeting: rational design. *Adv Mater* 2006;18:80–3.
- [9] Jung T, Kamm W, Breitenbach A, Kaiserling E, Xiao JX, Kissel T. Biodegradable nanoparticles for oral delivery of peptides: is there a role for polymers to affect mucosal uptake? *Eur J Pharm Biopharm* 2000;50:147–60.
- [10] Oh JK, Drumright R, Siegwart DJ, Matyjaszewski K. The development of microgels/nanogels for drug delivery applications. *Progr Polym Sci* 2008;33:448–77.
- [11] McAllister K, Sazani P, Adam M, Cho MJ, Rubinstein M, Samulski RJ, et al. Polymeric nanogels produced via inverse microemulsion polymerization as potential gene and antisense delivery agents. *J Am Chem Soc* 2002;124:15198–207.
- [12] Vinogradov SV, Bronich TK, Kabanov AV. Nanosized cationic hydrogels for drug delivery: preparation, properties and interactions with cells. *Adv Drug Deliv Rev* 2002;54:135–47.
- [13] Richardson TP, Peters MC, Ennett AB, Mooney DJ. Polymeric system for dual growth factor delivery. *Nat Biotechnol* 2001;19:1029–34.
- [14] Brekke JH, Thacker K. Hyaluronan as a biomaterial. In: Guelcher S, Hollinger JO, editors. Boca Raton: CRC Press; 2005. p. 219–40.
- [15] Burdick JA, Chung C, Jia XQ, Randolph MA, Langer R. Controlled degradation and mechanical behavior of photopolymerized hyaluronic acid networks. *Biomacromolecules* 2005;6:386–91.
- [16] Chen WYJ, Abatangelo G. Functions of hyaluronan in wound repair. *Wound Repair Regen* 1999;7:79–89.
- [17] Gupta P, Vermani K, Garg S. Hydrogels: from controlled release to pH-responsive drug delivery. *Drug Discov Today* 2002;7:569–79.
- [18] Leach JB, Bivens KA, Patrick CW, Schmidt CE. Photocrosslinked hyaluronic acid hydrogels: natural, biodegradable tissue engineering scaffolds. *Biotechnol Bioeng* 2003;82:578–89.
- [19] Luo Y, Ziebell MR, Prestwich GD. A hyaluronic acid-taxol antitumor bioconjugate targeted to cancer cells. *Biomacromolecules* 2000;1:208–18.
- [20] Mengher LS, Pandher KS, Bron AJ, Davey CC. Effect of sodium hyaluronate (0.1-percent) on break-up time (nibut) in patients with dry eyes. *Br J Ophthalmol* 1986;70:442–7.
- [21] Matyjaszewski K, Xia JH. Atom transfer radical polymerization. *Chem Rev* 2001;101:2921–90.
- [22] Tsarevsky NV, Bencherif SA, Matyjaszewski K. Graft copolymers by a combination of ATRP and two different consecutive click reactions. *Macromolecules* 2007;40:4439–45.
- [23] Wang JS, Matyjaszewski K. Controlled living radical polymerization – atom-transfer radical polymerization in the presence of transition-metal complexes. *J Am Chem Soc* 1995;117:5614–5.
- [24] Oh JK, Siegwart DJ, Matyjaszewski K. Synthesis and biodegradation of nanogels as delivery carriers for carbohydrate drugs. *Biomacromolecules* 2007;8:3326–31.
- [25] Siegwart DJ, Oh JK, Gao HF, Bencherif SA, Perineau F, Bohaty AK, et al. Biotin-, pyrene-, and GRGDS-functionalized polymers and nanogels via ATRP and end group modification. *Macromol Chem Phys* 2008;209:2180–93.
- [26] Jakubowski W, Matyjaszewski K. Activator generated by electron transfer for atom transfer radical polymerization. *Macromolecules* 2005;38:4139–46.
- [27] Oh JK, Tang CB, Gao HF, Tsarevsky NV, Matyjaszewski K. Inverse miniemulsion ATRP: a new method for synthesis and functionalization of well-defined water-soluble/cross-linked polymeric particles. *J Am Chem Soc* 2006;128:5578–84.
- [28] Bencherif SA, Srinivasan A, Horkay F, Hollinger JO, Matyjaszewski K, Washburn NR. Influence of the degree of methacrylation on hyaluronic acid hydrogels properties. *Biomaterials* 2008;29:1739–49.
- [29] Tsarevsky NV, Matyjaszewski K. Combining atom transfer radical polymerization and disulfide/thiol redox chemistry: a route to well-defined (bio)degradable polymeric materials. *Macromolecules* 2005;38:3087–92.
- [30] Xia JH, Matyjaszewski K. Controlled/“living” radical polymerization. Atom transfer radical polymerization using multidentate amine ligands. *Macromolecules* 1997;30:7697–700.
- [31] Lin-Gibson S, Bencherif S, Cooper JA, Wetzel SJ, Antonucci JM, Vogel BM, et al. Synthesis and characterization of PEG dimethacrylates and their hydrogels. *Biomacromolecules* 2004;5:1280–7.
- [32] Flory PJ. The principles of polymer chemistry. Ithaca, NY: Cornell University Press; 1953.
- [33] Rivlin RS. Large elastic deformations of isotropic materials.IV. Further developments of the general theory. *Philos Trans Roy Soc A* 1948;241:379–97.